Georeferenced gridded data handled by GMT: cartographic solutions for geophysical mapping

Polina LEMENKOVA[1,2]*

[1]Université Libre de Bruxelles, École Polytechnique de Bruxelles (Brussels Faculty of Engineering), Laboratory of Image Synthesis and Analysis (LISA)
[2]Schmidt Institute of Physics of the Earth, Russian Academy of Sciences. Department of Natural Disasters, Anthropogenic Hazards and Seismicity of the Earth. Laboratory of Regional Geophysics and Natural Disasters

*Correspondence to: Polina LEMENKOVA. E-mail: pauline.lemenkova@gmail.com.

Published:

1 November 2021

ABSTRACT: The functionality of Generic Mapping Tools (GMT) to process and visualize geospatial information is crucial to the development of the advanced cartographic method. This paper presents modelling and spatial analysis of the marine geological data using GMT shell scripting. GMT demonstrated effective cartographic solutions for visualization of the georeferenced data. The particular feature of GMT consists in its scripting modular approach that enables to use machine learning to explore reliable georeferenced data. Here, the study applies a sequential shell scripting to devise GMT modules for depicting marine geological data on the Mariana Trench. The data cover bathymetry, geophysics, tectonics and geology. The first method makes use of the 'nearneighbor' GMT module for grid contour modelling using Nearest Neighbor algorithm. This form of modelling classifies the geospatial data based on a similarity. The second method presents surface modelling from the initial XYZ-ASCII dataset by a combination of the 'blockmean' and 'surface' modules. The third method includes the use of the modules 'grdimage', 'psbasemap' and 'grdcontour' for plotting. Compared to GIS methods in which data are processed in a menu, GMT presents the console-based approach which automates cartographic data processing. The results present seven new maps and explanations of scripts.A combination of visual approaches applied using a color fill and various textures to represent data, which is effective in allowing readers to assess geophysical setting. The study demonstrated the effectiveness of GMT in geodata visualization.

KEY WORDS: cartography, machine learning, GMT, scripting, data analysis, data visualization.

1. Introduction

Geological studies are often being supported by GIS for modeling and mapping (Ayalew et al. 2005; Dixon, 2005; Gohl et al. 2006a, 2006b; Høyer et al. 2015; Arabameri et al. 2019; Andersen et al. 2020; Dulin, 2021). Maps often are designed by a specific software using available datasets.

Cartographic data contributing to these studies are being compiled using a wide range of methods and approaches. For example, geomorphic research of the hydrological effects on the location use GIS modeling and DEM analysis for geospatial or land cover analysis, environmental modelling, spatial metrics, geological mapping and other applications of ArcGIS (Berger et al, 2011; Suetova et al., 2005; Klaučo et al., 2013, 2017; Kuhn et al., 2006; Lemenkova et al., 2012). Mapping is usually using various available vector and raster databases preprocessed using standardized GIS solutions. Open repositories of the geodata are presented by GEBCO, ETOPO1 and SRTM widely used for mapping (Huvenne et al., 2011; Lemenkova, 2020b, c, d).

Published papers that describe and evaluate cartographic algorithms for data processing are diverse: application of aerial imagery, combined GIS based overlay of the topographic maps, photographs, and satellite images (Arróspide et al., 2018), regional change analysis (Marchese et al. 2017; Hudson et al., 2008), landslide susceptibility mapping (Bragagnolo et al. 2020; Basu and Pal, 2019). Mapmaking can include creating of series of maps that visualize environmental parameters of the studied objects. Integrated approaches of data processing include combined methods of field surveys, seismic profiles (Lemenkova, 2020a) echo sounding and classification of the satellite imagery (Ianniruberto et al., 2018; Lemenkova, 2011, 2015a). Other examples of GIS applications in mapping and geospatial research illustrate various technical approaches and methods for data analysis (Schenke and Lemenkova, 2008; Lemenkova, 2015b, 2019c; Gauger et al., 2007).

Despite the wide applicability of the traditional GIS, the workflow generally includes the sequence of various separated cartographic tasks required to create maps as making the workload overcomplicated and time-consuming. In contrast to GIS, scripting approach of cartographic techniques differs from those used for data processing by the traditional GIS. While GIS often requires operating single layers in a menu, adjusting map scales and projection for the whole GIS-project, creating specialized layouts using 'Layout Manager', and refining maintaining multiple settings in the graphical elements through the 'Properties' button, the Generic Mapping Toolset (GMT) enables to perform these adjustments in the 'on-the-fly' mode using a single script for each map, thus enabling fine tuning of the maps individually. In this way, scripting approach is much more flexible compared to the standard GIS software.

Scripting solutions for geospatial data modelling and visualization are diverse with the most reknown cartographic scripting toolset as GMT. The services of GMT scripting toolset, in particular, numerical data processing in various raw formats, a wide variety of modules designed and finely tuned for various operations on data, its compatibility with the utilities of GDAL (e.g. 'gdalinfo') and UNIX (e.g. 'echo'), expand the functionality of the GMT by allowing users who has certain skills in coding to produce print-quality maps. While some GIS do not enable to finely adjust most detailed cartographic elements (e.g. graticule, ticks, etc.) the GMT can produce sophisticated layouts using using specific modules by the advanced cartographic techniques where the data are visualized by using complex combination of GMT modules executed from a script. Besides GMT, they are also proposed by the GRASS GIS (Lemenkova, 2020g, 2020h), R of Python scripting libraries (Lemenkova, 2018a; 2018b; 2019f), AWK (Lemenkova, 2019g). The variety of these examples proves scripting to be effective tool for the cartographic visualization and data analysis.

2. Study area

The study area (Fig. 1) located in west Pacific Ocean, the Mariana Trench located in the western part of the Pacific Ocean on the border of two major tectonic plates: Pacific and Philippine (Fig. 2).

The analyzed grids were situated in the area with aim to visualize spatial variations in the geophysical settings by methods of spatial analysis using technical means of GMT. Mariana Trench is the deepest place on the Earth with unique geological settings. Advanced research papers have been reported various aspects of the Marian Trench geology, bathymetry and oceanological setting (Fryer et al., 2003; Gallo et al., 2015; Curtis and Moyer, 2005; Gooday et al. 2008; Lemenkova, 2019a, b, c; Fujioka et al., 2002; Hand et al., 2020).
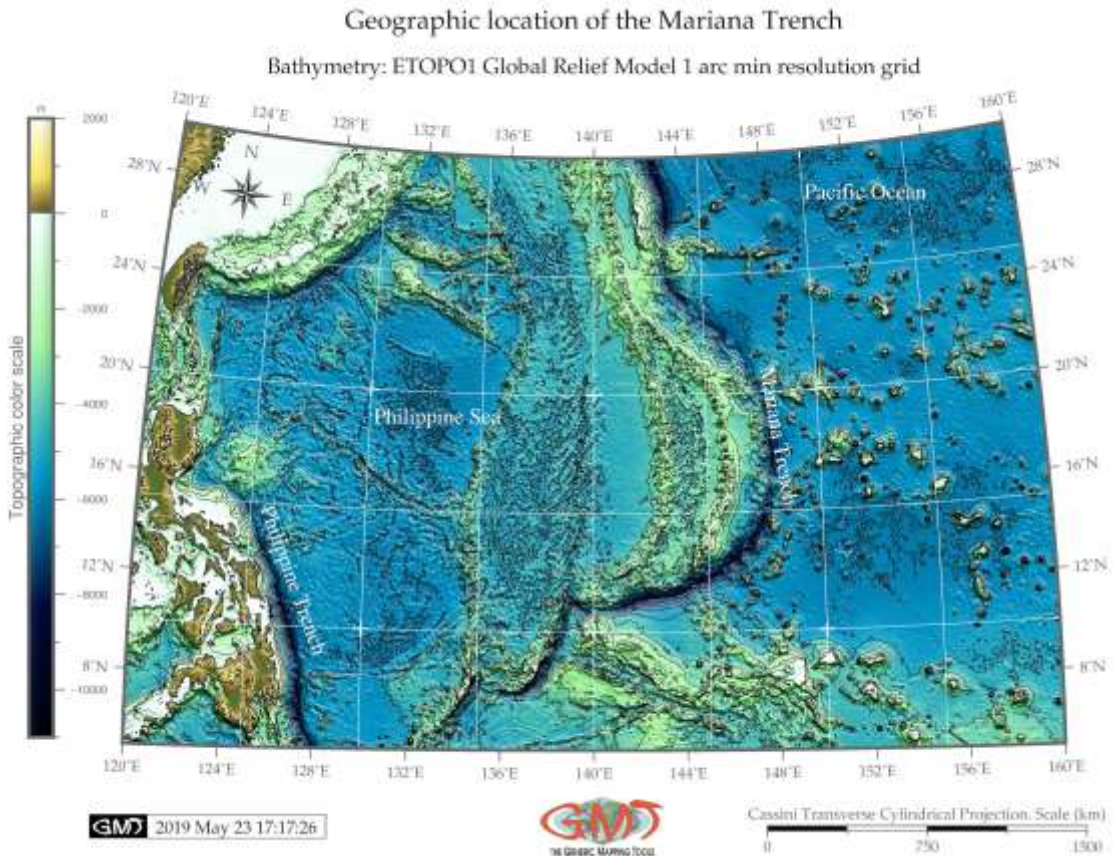

Figure 1 Bathymetric map of the Mariana Trench. Data: ETOPO1. Mapping: GMT.

The tectonic conditions of the trench are highly complex which is explained by the location in the region of high seismicity, volcanism, extent of the faults and hot spots in the nearby area (Fig. 3). For instance, the Philippine fault, one of the major strike-slip faults of the world, extending from the Lingayen-La Union (NW Luzon) to the Davao Gulf (Southern Mindanao) is located in the region of the Philippine Sea, west of the Mariana Trench (Bischke et al., 1990). Besides the tectonic setting of the trench, the geology of the west Pacific has undergone a long process of evolution. As a result, the area of the Mariana Trench is located in the subduction zone of the tectonic plates (Hall et al., 1995) and is affected by various geological processes: metamorphic reactions, fluid and melt transfer and earthquakes which occur at a subducting zone (Bessat et al., 2020). As a deep-sea trench, Mariana Trench occurs special geophysical setting such as geoid anomaly which

increases in height as it approaches the trench axis from the seaward side (Chapman and Talwani, 1982).
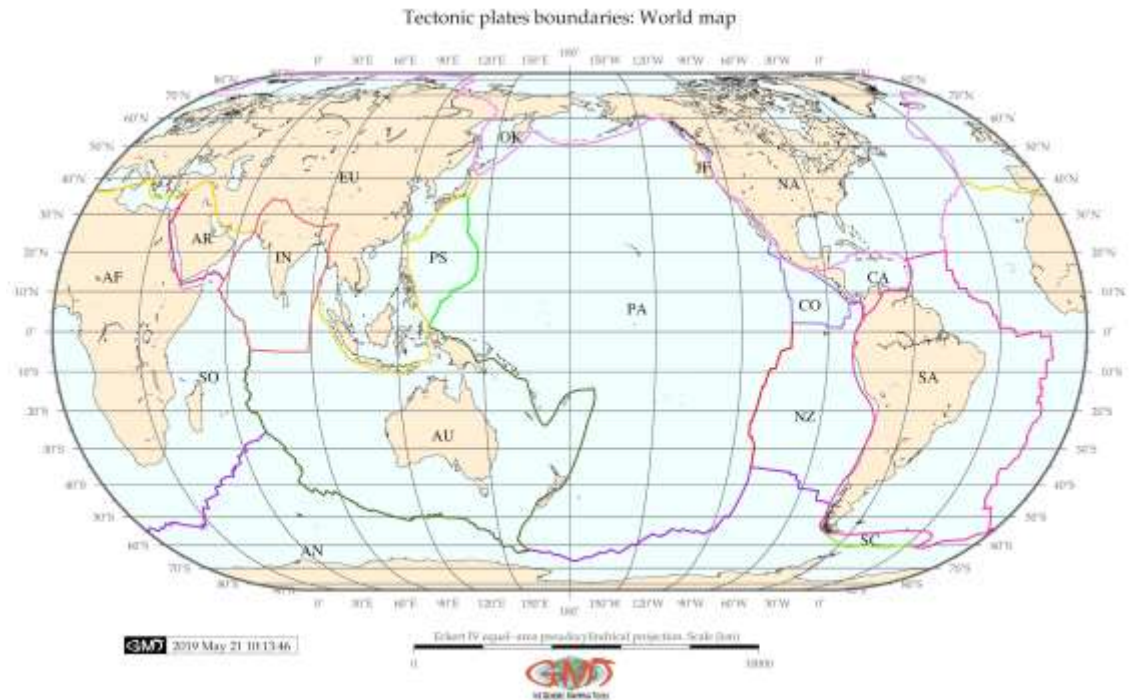

Figure 2 Tectonic provinces on the Pacific Ocean. Data compiled after: Coffin et al. (1998), Bird (2003). Mapping: GMT.

The region is divided into the multiple provinces in the west and volcanic units overlying metamorphic rocks in the basement and ophiolites in the east (Fig. 3). Therefore, the relief of the Mariana Trench was formed under the impact of a variety of processes and setting discussed in relevant publications (Bird, 1978; Fryer, 1996; Fouch and Fischer, 1998; Shiobara et al., 2010; Bentham and Rost, 2014; Carvallo et al., 2017).

3. Methods

Methodology of the current research included scripting techniques of the GMT used for visualization and modelling (Wessel and Smith, 1995) by the existing methodology (Lemenkova, 2020e, 2020f). Data covering study area included raster layers on the following clusters: geology, bathymetry (ETOPO1 1), gravity and topography data sets from global 1-minute grids in ASCII XYZ-format derived by selecting proper coordinates for the current project (East extent: 144-162; North extent: 40-51): http://topex.ucsd.edu/cgi-bin/get_data.cgi.

3.1. Grid contour modelling using Nearest Neighbor algorithm

Grid contour modelling for visualization of the topography (Fig. 4), was performed in GMT using the following modules: gmtset, gmtdefaults, gmtinfo, gmtconvert, nearneighbor, grdcontour,

pscoast, pstext, gmtlogo, psconvert. Plotting contour gives the background for further GIS techniques discussed in previous works (Lemenkova, 2019d; 2019e), allowing to check up for the patterns of the bathymetric data, and analyzing the morphologic shape of the trench.
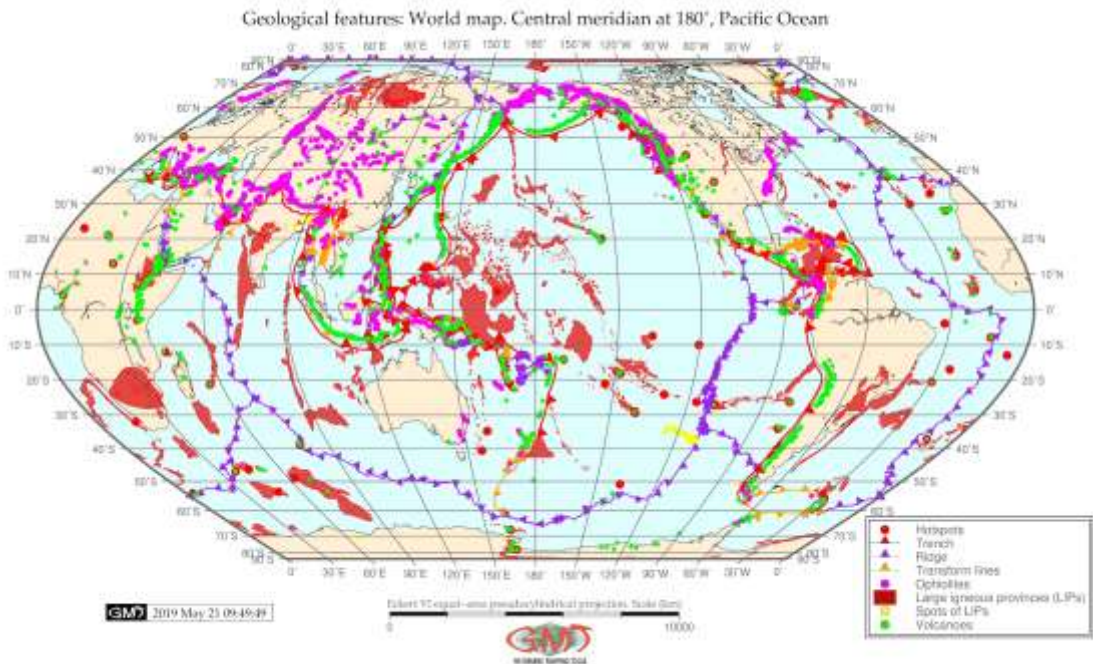

Figure 3 Geologic features and lineaments of the Pacific Ocean: Ophiolites compiled by PLATES, primarily from the Exxon tectonic maps (Exxon Production Research Company (World Mapping Project), 1985). Large Igneous Provinces (LIPs) from Coffin et al. (2006); tectonic plates and lineaments: trench, ridge, transform lines (Coffin et al. 1998). Present-day hotspot locations. Data: ophiolites (Mann and Taira, 2004). Mapping: GMT.

The presented model (Fig. 4) was done using the Nearest Neighbor method by module 'nearneighbor' applying the following GMT script:
# Step-1. Generating file
ps=GMT_NNgrid_MT.ps
# Step-2. Gridding using a nearest neighbor technique
region=`gmt info topo_MT.b -I1 -bi3d`
gmt nearneighbor $region -I10m -S40k -Gtopo_NN_MT.nc topo_MT.b -bi
Step-3. Add contour lines
gmt grdcontour topo_NN_MT.nc -R120/160/5/30 -JM6i -P -C1000 -A2000+f6p,Times-Roman -Gd2i -K > $ps
Step-4. Add coastline
gmt pscoast -R -J -P   -Bpxg4f2a4 -Bpyg4f2a4 -Bsxg2 -Bsyg2 -Df -Wthinnest -B+t"Grid contour modelling using Nearest Neighbor algorithm. Mariana Trench area"   -TdjBR+w0.4i+l+o0.15i   -Lx13.0c/-1.1c+c50+w800k+l"Mercator projection, Scale, km"+f -UBL/-15p/-35p -O -K >> $ps
Step-5. Convert to image file using GhostScript (portrait orientation, 720 dpi)

gmt psconvert GMT_NNgrid_MT.ps -A0.2c -E720 -Tj -P -Z

Contouring grid from the XYZ ASCII data enables to visualize the bathymetry from the raw data and represent a base map schematically showing the bathymetry of the study area (Fig. 4).
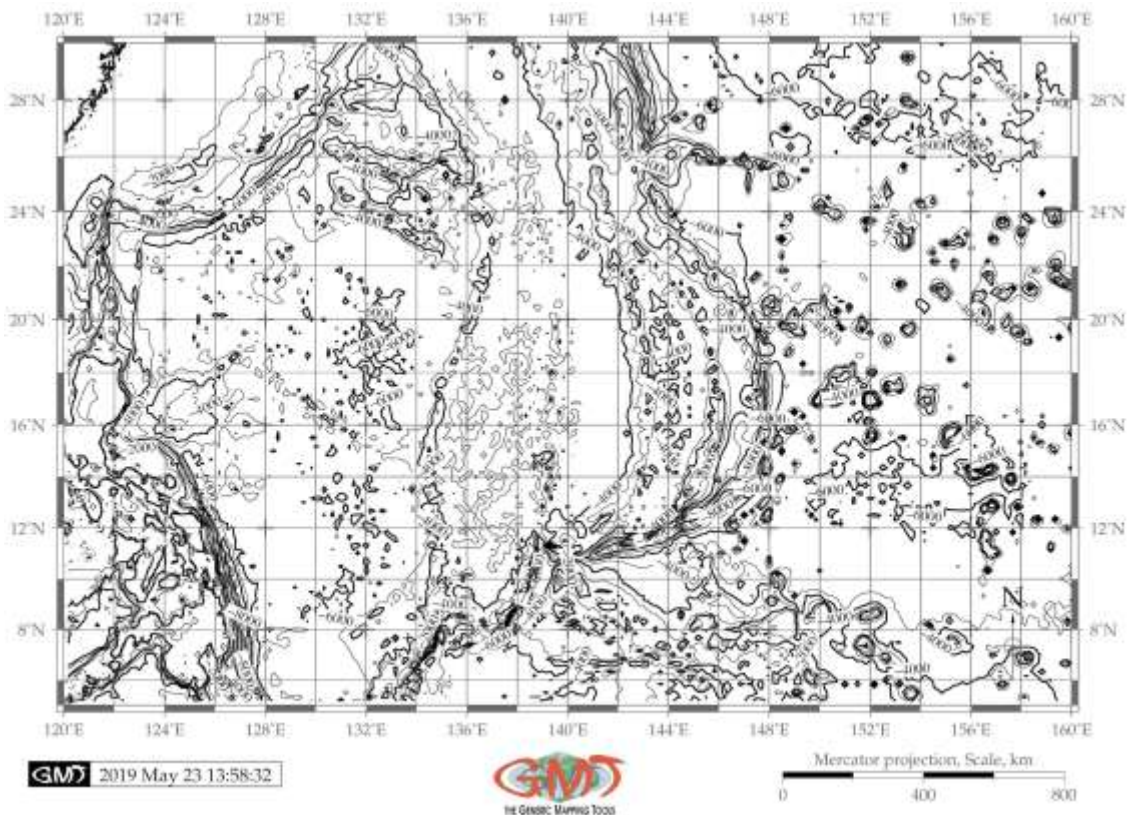

Figure 4 Grid contour modelling using the Nearest Neighbor algorithm applied for the Mariana Trench area and the Philippine Sea (depth measured in meters). Input table data: global 1-min grid resolution in ASCII XYZ-format, converted to binary format. Mapping: GMT.

3.2. Topographic surface modelling from the initial XYZ-ASCII data set

The next step included surface modelling by 'surface' module of GMT illustrated on Fig. 5.

Modelling was implemented by the following key algorithm of the GMT:
Step-1. Generate 1 by 1 minute block mean values from the raw ASCII data (xyg table)
gmt blockmean topo_MT.xyz -R120/160/5/30 -I1m -Vv > topo_MT_BM.xyg
Step-2. Generate grid from xyz table format
gmt surface topo_MT_BM.xyg -R120/160/5/30 -T0.25 -I30s -GSurface_MT.nc -Vv
Step-3. Make gradient illumination with azimuth 45 degree
gmt grdgradient Surface_MT.nc -GSurface_MT.int -A0/45 -Ne1 -fg
Step-4. Make raster image
gmt grdimage Surface_MT.nc -CsurfaceMT.cpt -R120/160/5/30 -JM6i -P -ISurface_MT.int -Xc -K > $ps

Step-5. Add grid
gmt psbasemap -R -J -Bpxg6f2a2 -Bpyg6f1a2 -Bsxg2 -Bsyg2 -B+t"Surface modelling of the topography along the Mariana Trench" -O -K >> $ps
Step-6. Convert to image file using GhostScript
gmt psconvert SurfaceTMT.ps -A0.2c -E720 -P -Tj -Z

Additional cartographic elements, GMT logo, color scale and aesthetics were added using the following modules: gmtset, gmtdefaults, makecpt, gmtinfo, blockmean, surface, grdgradient, grdimage, psbasemap, psscale, gmtlogo, pstext, psconvert. Surface model displays the values for the topographic variables (depths and heights) modeled from the raw ASCII XYZ data set format with applied blockmean filter as a smoothing factor. The cartographic output of the model shows (Fig. 5) high resolution raster grid (30 seconds) in the netCDF format, converted to the jpg.
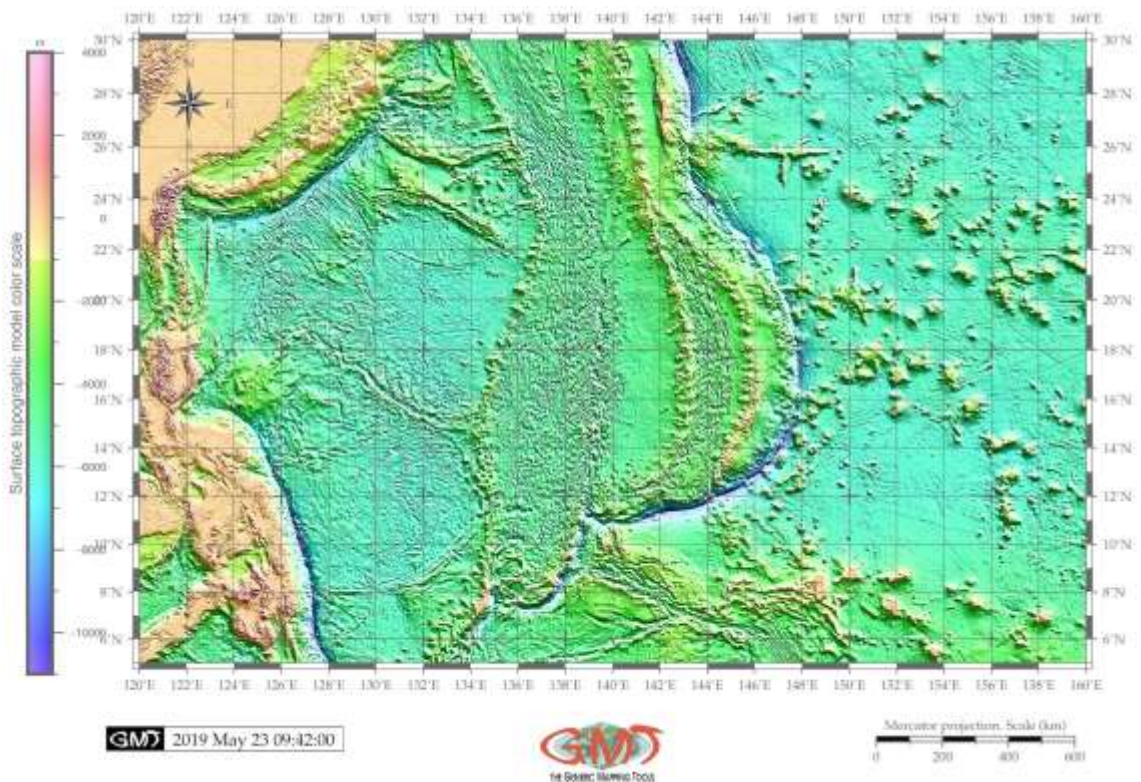

Figure 5 Surface modelling of the topography of the Mariana Trench. Modelling: GMT module 'surface', tension factor of the continuous curvature splines 0.25. Input raw table data: global 1-min grid resolution in ASCII XYZ-format, applied blockmode filter. Output spatial model: 30-sec grid spacing in NetCDF format, shading azimuth gradient: 45°. Mapping: GMT.

Shading azimuth gradient is set to the 45°, that is, illumination is located on the NE. The model gives an inside into the bathymetry as a high-resolution grid map showing the continuous depths and heights as colors, which is more effective comparing to contouring. Based on the topographic model (Fig. 5) it can be roughly determined that that shape of the Mariana Trench approximates a

geometric crescent. Surface modelling provided by GMT is one of the advantageous approach for the geospatial data modelling from the initial raw XYZ-ASCII table.

3.3. Geoid raster image modelling from the XYZ data set, GMT

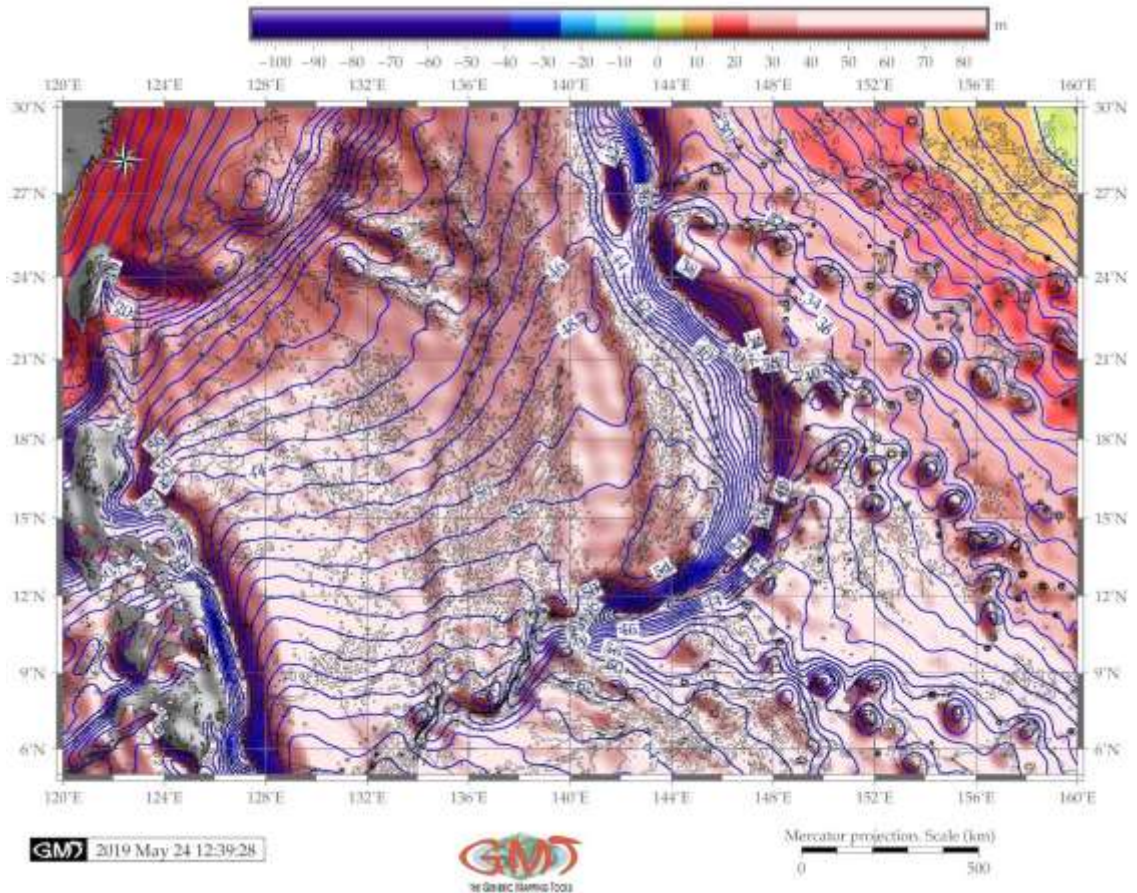Another method used in this geospatial data analysis was modelling geoid (Fig. 6).

Figure 6 Color surface modelling of geoid along the Mariana Trench with gray-shaded topography of the clipped land areas. Modelling: GMT module 'surface', tension factor of the continuous curvature splines 0.25. Raw table data: global 1-min grid in ASCII XYZ-format, applied blockmode filter. Output spatial model: 30-sec grid spacing in NetCDF. Mapping: GMT.

Geoid model (Fig. 6) represents a map showing the shape that the surface of the ocean would have with the only influence of the gravity and rotation of Earth provided other meteorological influences (e.g. winds, tides) are absent. The data as a grid raster (geoid.egm96.grd) was visualized and then the land areas were clipped as the gray-shaded areas to focus on the ocean. The model implies the graphical representation of the geoid data ranging from -110 to -90 mGal, where the majority of the data range (represented in red colors) lies in the interval of 20-80 mGal. The geoid modelling with high accuracy is a major issue in physical geodesy and oceanography (Sandwell and

Smith, 1997). The numbers give the degree of the leveling geoid heights ranges. In the shaded colors, each color is given the assigned color according to the 'haxby' color palette, used by W. F. Haxby's Gravity field of World's oceans, 1985, developed for geoid and gravity maps. Each color, as explained in the color legend on the top of the map, is subdivided into sub-classes (violet, blue, green, orange, red), ranging from -110 to 90 mGal (Fig. 6).

Modelling was done using following snippet GMT shell script:

```
# Step-1. Generate geoid image with coloring and contour
gmt grd2cpt geoid.egm96.grd -Chaxby > geoid.cpt
gmt grdimage geoid.egm96.grd -I+a45+nt1 -R120/160/5/30 -JM6.5i -Cgeoid.cpt -P -K > $ps
gmt grdcontour geoid.egm96.grd -R -J -C2 -A2+f8p+gwhite -Wthin,blue -O -K >> $ps
# Step-2. Use gmt pscoast to initiate clip path for land
gmt pscoast -R120/160/5/30 -J -Dh -Gc -O -K >> $ps
# Step-3. Generate topography image with shading
gmt makecpt -C150 -T-11000,2000 -N > shadeMT.cpt
gmt grdimage geoid.egm96.grd -I+a45+nt1 -R -J -CshadeMT.cpt -O -K >> $ps
# Step-4. Clipping and overlay basemap
gmt pscoast -R -J -O -K -Q -B+t"Color geoid image of the Mariana Trench with gray-shaded topography of the clipped land areas" >> $ps
# Step-5. Add shorelines
gmt grdcontour mt_relief.nc -R -J -C1000 -O -K >> $ps
# Step-6. Add grid
gmt psbasemap -R -J -Bpxg8f2a4 -Bpyg6f3a3 -Bsxg4 -Bsyg3 -O -K >> $ps
# Step-7. Put a color legend on top of the land mask
gmt psscale -DjTC+o0.8c/-1.6c+w12c/0.5c+h -R -J -Cgeoid.cpt -Bx10f1 -By+lmGal -I -O -K >> $ps
# Step-8. Adding GMT logo
gmt logo -Dx6.2/-2.2+o0.1i/0.1i+w2c -O >> $ps
# Step-9. Convert to image file using GhostScript
gmt psconvert GMT_clip_MT.ps -A0.2c -E720 -Tj -P -Z
```

3.4. Gravimetric surface modelling

Gravimetric surface modelling (Fig. 7) shows visualized and modeled data from the satellite gravimetry, following the Global Positioning System (GPS) development in the field of geodesy and altimetry. Tension factors of the splines was selected as 0.25 (from the possible values of 0 to 1) as the best approximating the curvature of the splines. Spatially coincident data on the trench (bathymetry, geoid and gravity) were plotted in the same projection to facilitate comparison.

The input raw data were taken from the available online website (http://topex.ucsd.edu/cgi-bin/get_data.cgi) with selected coordinate range of the East-144-162 degrees, North: 40-51 degrees. The records of the gravimetric data were modeled using the following GMT code snippet:

```
# Step-1. Generate 1 by 1 minute block mode values from the raw ASCII data (xyg table)
gmt blockmode grav_MT.xyz -R120/160/5/30 -I1m -Vv > grav_MT_BM.xyg
# Step-2. Generate grid from xyz table format
gmt surface grav_MT_BM.xyg -R120/160/5/30 -T0.25 -I30s -GSurfaceG_MT.nc -Vv
# Step-3. Make raster image
gmt grdimage SurfaceG_MT.nc -CsurfMTgrav.cpt -R120/160/5/30 -JM6i -P -I+a15+ne0.75 -Xc -K > $ps
# Step-4. Add grid
```

gmt psbasemap -R -J -Bpxg8f2a2 -Bpyg4f2a2 -Bsxg4 -Bsyg4 -B+t"Surface modelling of the gravity along the Mariana Trench" -O -K >> $ps

Step-5. Add scale, directional rose

gmt psbasemap -R -J -Tdx0.8c/9.0c+w0.3i+f2+l+o0.0c -Lx5.3i/-0.5i+c50+w400k+l"Mercator projection. Scale (km)"+f -UBL/-15p/-40p -O -K >> $ps

Step-6. Add color legend

gmt psscale -R -J -CsurfMTgrav.cpt -Dg120/4+w10c/0.4c+v+o-1.8/0.2c+ml -Baf+l"Surface gravimetric model color scale" -I0.2 -By+lmGal -O -K >> $ps

Step-7. Convert to image file using GhostScript

gmt psconvert SurfaceGMT.ps -A0.2c -E720 -P -Tj -Z

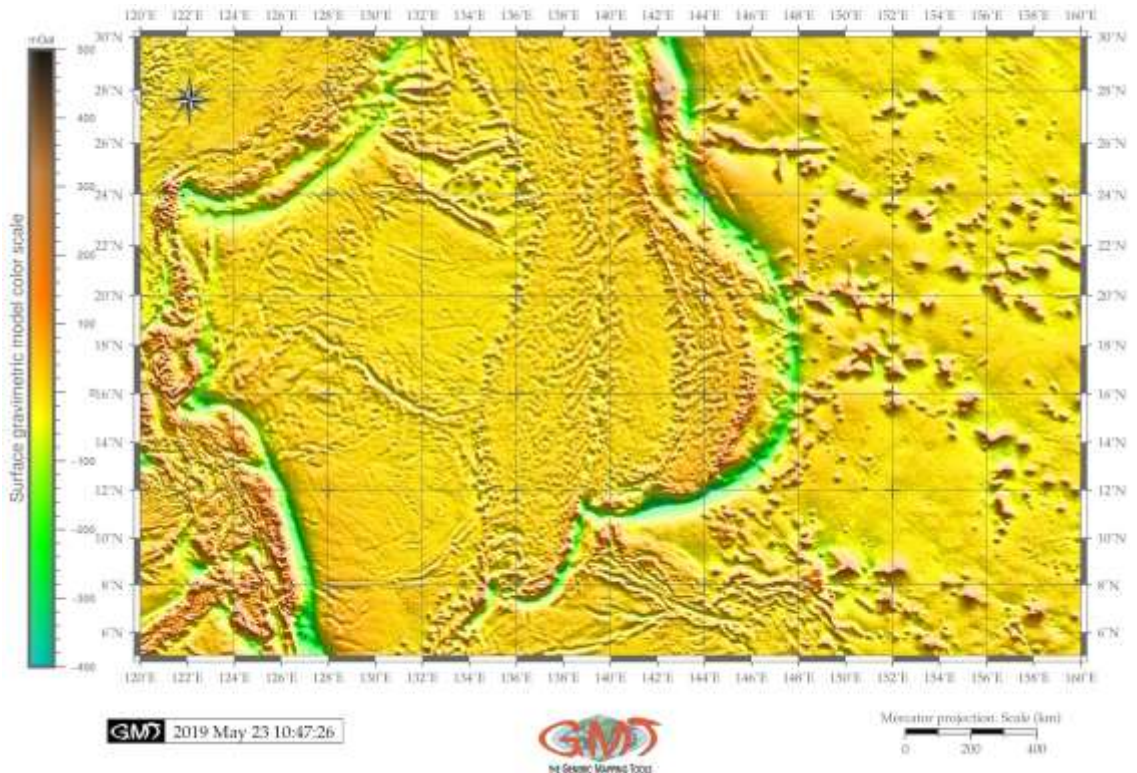The output map is shown on the Fig. 7.

Figure 7 Color surface modelling of the gravity along the Mariana Trench. Modelling: GMT module 'surface', tension factor of the continuous curvature splines 0.25. Input raw table data: global 1-min grid resolution in ASCII XYZ-format, applied blockmode filter. Output spatial model: 30-sec grid spacing in NetCDF format. Mapping: GMT.

Gravimetric observation values are modeled with the 30-sec output grid resolution in cells contained in a matrix and represented as colors. The color palette located on the left of the map shows the range of the gravimetry data starting from -400 to 500 mGal, with colors grouped based on the similarity of the values. The color palette was selected as 'elevation', with the deepest values are visualized as green values, and vice versa, the highest as brown.

4. Results and discussion

This study demonstrated the GMT applicability for cartographic visualization of the geophysical settings of the Mariana Trench. The gravity and geoid modelling gives a response towards the geodetic location, gravimetric properties of the place by steepness of the gradient and depth. The bathymetric patterns of the submarine trench change in space gradually due to the preconditioning by the mentioned above factors. It is also highly sensitive to the trigger factors, such as tectonic development and plate subduction that contribute towards hadal sedimentation, and accounting for the topographic variability. Changes in the directions and intensity of the deep-sea current brought on by external factors, such as the submarine volcanism, may cause increase of the sedimentation proving a feedback mechanism between the marine geological and biological factors. In turn, this affects the geomorphic properties of the trench. Such a feedback mechanism should be observed as a recommendation for further studies based on the available data derived from the direct cruise observations. Submarine sedimentation in the deep-sea trenches spatially correlate not only to the geological and tectonic factors of the specific trench, but also to its deformation features that induce the volcanism and closeness of the large igneous volcanic provinces. In such cases, the sedimentation response to these factors is a rapid process that gradually changes the geomorphic form of the trench.

Deep-sea trenches are important geomorphological forms in the ocean system (De Leo et al., 2010). They may be approximated to the tributary river flows as channels for the flow of turbidity currents across the seafloor. The fine-grained sediments, e.g. clay and silt, are deposited from the turbidity currents channeled from the continental margins along the submarine canyons down into deep ocean trenches. Hence, the interconnectivity between various parts of the ocean submarine geomorphology is very complex which requires a numerical approach in studies. Therefore, as a recommendation for future studies, additional data should be used for modeling the seafloor based on the availability. The actuality of this research consists in its technical presentation of the shell scripts of GMT with comments, explanation and direct snippets, which enables a cross-disciplinary approach that combines traditional GIS methods of data visualization with geospatial analysis of the study area performed in GMT. Presented shell scripts of the GMT provided in this paper are intended for possible future replications in similar studies. Mixed combination of the geological analysis and GIS visualization with syntax of shell scripting is shown in this paper.

5. Conclusion

Rapid development of methods of the geospatial data processing has recently grown across a variety of Earth science disciplines: geology, cartography, meteorology, environmental monitoring and land use/cover studies. However, the use of the high-level cartographic toolset GMT based on shell scripting in the domain of the marine geology was not discussed and presented in the existing literature in full, with code snippets, as it is required by coding. Therefore, introducing scripting cartographic methods in the marine geology requires special focus and attention as lacking comprehensive introduction of the machine learning algorithms in geoscience domains.

Heretofore, current state of the research in Earth science domains included various computing methods supported mainly by the traditional GIS. While some work fragmentary include shell scripts as plugins, relatively few GIS works use scripting approach or programming languages, however the most of research is still based on the traditional GIS (e.g. ArcGIS). On the other hand,

supporting shell scripting in cartographic routine for raster grids visualization modelling would contribute significantly towards the development of technical cartographic progress in GIS. In view of this, current paper contributes to the technical cartographic development in geoscience.

The novelty of the GMT approach consists in the highlighting of the shell scripting functionality and applicability. Using machine learning algorithms in the cartographic routine is crucial in Earth science for georeferenced data processing, doing a step apart from the traditional GIS. Practical purpose of this work was, therefore, to demonstrate the selected modules of the GMT for the marine geological data modeling and visualization. Effective and precise plotting supported by GMT, demonstrated its indisputable advantages and applicability of UNIX in cartography.

Acknowledgements

References

Andersen, T.R., Poulsen, S.E., Pagola, M.A., Medhus, A.B. 2020. Geophysical mapping and 3D geological modelling to support urban planning: A case study from Vejle, Denmark. Journal of Applied Geophysics, 180, 104130. https://doi.org/10.1016/j.jappgeo.2020.104130.

Anderson, R.N. 1975. Heat flow in the Mariana Marginal Basin. Journal of Geophysical Research, 80(29), 4043–4048. https://doi.org/10.1029/JB080i029p04043.

Arabameri, A., Pradhan, B., Rezaei, K., Conoscenti, C. 2019. Gully erosion susceptibility mapping using GIS-based multi-criteria decision analysis techniques. Catena, 180, 282–297. https://doi.org/10.1016/j.catena.2019.04.032.

Arróspide, F., Mao, L., Escauriaza, C. 2018. Morphological evolution of the Maipo River in central Chile: Influence of instream gravel mining. Geomorphology, 306, 182–197. https://doi.org/10.1016/j.geomorph.2018.01.019.

Ayalew, L., Yamagishi, H. Marui, H., Kanno, T. 2005. Landslides in Sado Island of Japan: Part II. GIS-based susceptibility mapping with comparisons of results from two methods and verifications. Engineering Geology, 81(4), 432-445. https://doi.org/10.1016/j.enggeo.2005.08.004.

Basu, T., Pal, S. 2019. RS-GIS based morphometrical and geological multi-criteria approach to the landslide susceptibility mapping in Gish River Basin, West Bengal, India. Advances in Space Research, 63(3), 1253-1269. https://doi.org/10.1016/j.asr.2018.10.033.

Bechter, T., Baumann, K., Birk, S., Bolik, F., Graf, W., Pletterbauer, F. 2018. LaRiMo – A simple and efficient GIS-based approach for large-scale morphological assessment of large European rivers. Science of the Total Environment, 628–629, 1191–1199. https://doi.org/10.1016/j.scitotenv.2018.02.084.

Bentham, H.L.M., Rost, S. 2014. Scattering beneath Western Pacific subduction zones: evidence for oceanic crust in the mid-mantle. Geophysical Journal International, 197(3), 1627–1641. https://doi.org/10.1093/gji/ggu043.

Berger, J.-F. 2011. Hydrological and post-depositional impacts on the distribution of Holocene archaeological sites: The case of the Holocene middle Rhône River basin, France. Geomorphology, 129, 167–182. https://doi.org/10.1016/j.geomorph.2011.02.021.

Bessat, A., Duretz, T., Hetényi, G., Pilet, S., Schmalholz, S.M. 2020. Stress and deformation mechanisms at a subduction zone: insights from 2-D thermomechanical numerical

modelling. Geophysical Journal International, 221(3), 1605–1625. https://doi.org/10.1093/gji/ggaa092.

Bird, P. 1978. Stress and temperature in subduction shear zones: Tonga and Mariana. Geophysical Journal International, 55(2), 411–434. https://doi.org/10.1111/j.1365-246X.1978.tb04280.x.

Bird, P. 2003. An updated digital model of plate boundaries. Geochemistry, Geophysics, Geosystems, 4(3), 1027. https://doi.org/10.1029/2001GC000252.

Bischke, R.E., Suppe, J., Del Pilar, R. 1990. A new branch of the Philippine fault system as observed from aeromagnetic and seismic data. Tectonophysics, 183, 243–264. https://doi.org/10.1016/0040-1951(90)90419-9.

Bragagnolo, L., da Silva, R.V., Grzybowski, J.M.V. 2020. Landslide susceptibility mapping with r.landslide: A free open-source GIS-integrated tool based on Artificial Neural Networks. Environmental Modelling & Software, 123, 104565. https://doi.org/10.1016/j.envsoft.2019.104565.

Carvallo, C., Camps, P., Sager, W.W., Poidras, T. 2017. Palaeointensity determinations and magnetic properties on Eocene rocks from Izu-Bonin-Mariana forearc (IODP Exp. 352), Geophysical Journal International, 210(3), 1993–2009. https://doi.org/10.1093/gji/ggx208.

Chapman, M.E., Talwani, M. 1982. Geoid anomalies over deep sea trenches. Geophysical Journal International, 68(2), 349–369. https://doi.org/10.1111/j.1365-246X.1982.tb04905.x.

Coffin, M.F., Gahagan, L.M., Lawver, L.A. 1998. Present-day Plate Boundary Digital Data Compilation. University of Texas Institute for Geophysics Technical Report, 174, pp. 5.

Coffin, M.F., Duncan, R.A., Eldholm, O., Fitton, J.G., Frey, F.A., Larsen, H.C., Mahoney, J.J., Saunders, A.D., Schlich, R., Wallace, P.J. 2006. Large igneous provinces and scientific ocean drilling: Status quo and a look ahead. Oceanography, 19(4), 150–160. https://doi.org/10.5670/oceanog.2006.13.

Curtis, A.C., Moyer, C.L. 2005. Mariana forearc serpentinte mud volcanoes harbor novel communities of extremophilic ArchaeaJ. Geomicrobiology Journal 30(5), 430–441. https://doi.org/10.1080/01490451.2012.705226.

De Leo, F.C., Smith, C.R., Rowden, A.A., Bowden, D.A., Clark, M.R. 2010. Submarine canyons: hotspots of benthic biomass and productivity in the deep sea. In: Proceedings of the Royal Society B (277), 2783–2792. https://doi.org/10.1098/rspb.2010.0462.

Dixon, B. 2005. Groundwater vulnerability mapping: A GIS and fuzzy rule based integrated tool. Applied Geography, 25(4), 327–347. https://doi.org/10.1016/j.apgeog.2005.07.002.

Dulin, S.A. 2021. Geologic Field Methods and Mapping. Editor(s): Alderton, D., Elias, S.A. Encyclopedia of Geology (2nd Ed.). Academic Press, 294–300. https://doi.org/10.1016/B978-0-12-409548-9.12544-8.

Exxon Production Research Company (World Mapping Project) 1985. Tectonic Map Series of the World, Exxon Production Research Company, Houston, TX.

Fouch, M.J., Fischer, K. M. 1998. Shear wave anisotropy in the Mariana Subduction Zone. Geophysical Research Letters, 25(8), 1221–1224. https://doi.org/10.1029/98GL00650.

Fryer, P., Becker, N., Appelgate, B., Martinez, F., Edwards, M., Fryer, G. 2003. Why is the Challenger Deep so deep? Earth and Planetary Science Letters, 211(3–4), 259–269. https://doi.org/10.1016/S0012-821X(03)00202-4.

Fryer, P. 1996. Evolution of the Mariana Convergent Plate Margin System. Reviews of Geophysics, 34(1), 89– 125. https://doi.org/10.1029/95RG03476.

Gallo, N.D., Cameron, J., Hardy, K., Fryer, P. Bartlett, D.H., Levin, L.A. 2015. Submersible- and lander-observed community patterns in the Mariana and New Britain trenches: Influence of

productivity and depth on epibenthic and scavenging communities. Deep Sea Research Part I: Oceanographic Research Papers, 99, 119–133. https://doi.org/10.1016/j.dsr.2014.12.012.

Gauger, S., Kuhn, G., Gohl, K., Feigl, T., Lemenkova, P., Hillenbrand, C.-D. 2007. Swath-bathymetric mapping. In Gohl, K. The expedition ANTARKTIS-XXIII/4 of the Research Vessel 'Polarstern' in 2006. Reports on Polar and Marine Research, 557, 38–45. https://doi.org/10.6084/m9.figshare.7439231.

Gohl, K., Eagles, G., Udintsev, G., Larter, R. D., Uenzelmann-Neben, G., Schenke, H.-W., Lemenkova, P., Grobys, J., Parsiegla, N., Schlueter, P., Deen, T., Kuhn, G., Hillenbrand, C.-D. 2006a. Tectonic and sedimentary processes of the West Antarctic margin of the Amundsen Sea embayment and PineIsland Bay, 2nd SCAR Open Science Meeting, 12-14 Jul, Hobart, Australia. https://doi.org/10.6084/m9.figshare.7435484.

Gohl, K., Uenzelmann-Neben, G., Eagles, G., Fahl, A., Feigl, T., Grobys, J., Just, J., Leinweber, V., Lensch, N., Mayr, C., Parsiegla, N., Rackebrandt, N., Schlüter, P., Suckro, S., Zimmermann, K., Gauger, S., Bohlmann, H., Netzeband, G., Lemenkova, P. 2006b. Crustal and Sedimentary Structures and Geodynamic Evolution of the West Antarctic Continental Margin and Pine Island Bay. Expeditionsprogramm Nr. 75 ANT XXIII/4 ANT XXIII/5, 11–12. https://doi.org/10.13140/RG.2.2.16473.36961.

Gooday, A.J., Todo, Y., Uematsu, K., Kitazato, H. 2008. New organic-walled Foraminifera (Protista) from the ocean's deepest point, the Challenger Deep (western Pacific Ocean). Zoological Journal of the Linnean Society, 153, 399-423. https://doi.org/10.1111/j.1096-3642.2008.00393.x.

Hall, R., Ali, J.R., Anderson, C.D., Baker, S.J. 1995. Origin and motion history of the Philippine Sea Plate. Tectonophysics, 251(1–4), 229-250. https://doi.org/10.1016/0040-1951(95)00038-0.

Hand, K.P., Bartlett, D.H., Fryer, P., Peoples, L., Williford, K., Hofmann, A.E., Cameron, J. 2020. Discovery of novel structures at 10.7 km depth in the Mariana Trench may reveal chemolithoautotrophic microbial communities. Deep Sea Research Part I: Oceanographic Research Papers, 160, 103238. https://doi.org/10.1016/j.dsr.2020.103238.

Høyer, A.-S., Jørgensen, F., Sandersen, P.B.E., Viezzoli, A., Møller, I. 2015. 3D geological modelling of a complex buried-valley network delineated from borehole and AEM data. Journal of Applied Geophysics, 122, 94-102. https://doi.org/10.1016/j.jappgeo.2015.09.004.

Hudson, P.F., Middelkoop, H., Stouthamer, E. 2008. Flood management along the Lower Mississippi and Rhine Rivers (The Netherlands) and the continuum of geomorphic adjustment. Geomorphology, 101, 209–236. https://doi.org/10.1016/j.geomorph.2008.07.001.

Ianniruberto, M., Trevethan, M., Pinheiro, A., Andrade, J.F., Dantas, E., Filizola, N., Santos, A., Gualtieri, C. 2018. A field study of the confluence between Negro and Solimoes Rivers. Part 2: Bed morphology and stratigraphy. Comptes Rendus Geoscience, 350, 43–54. https://doi.org/10.1016/j.crte.2017.10.005.

Huvenne, V.A.I., Tyler, P.A., Masson, D.G., Fisher, E.H., Hauton, C., Hühnerbach, V., Bas, T.P.L., Wolff, G.A. 2011. A Picture on the Wall: Innovative Mapping Reveals Cold-Water Coral Refuge in Submarine Canyon. PlosOne 6(12), 1–9. https://doi.org/10.1371/journal.pone.0028755.

Klaučo, M., Gregorová, B., Stankov, U., Marković, V., Lemenkova, P. 2013. Determination of ecological significance based on geostatistical assessment: a case study from the Slovak Natura 2000 protected area. Central European Journal of Geosciences, 5(1), 28–42.

Klaučo, M., Gregorová, B., Stankov, U., Marković, V., Lemenkova, P. 2017. Land planning as a support for sustainable development based on tourism: A case study of Slovak Rural Region. Environmental Engineering and Management Journal, 2(16), 449–458.

Kuhn, G., Hass, C., Kober, M., Petitat, M., Feigl, T., Hillenbrand, C. D., Kruger, S., Forwick, M., Gauger, S., Lemenkova, P. 2006. The response of quaternary climatic cycles in the South-East Pacific: development of the opal belt and dynamics behavior of the West Antarctic ice sheet. In: Gohl, K. (ed). Expeditionsprogramm Nr. 75 ANT XXIII/4, AWI.

Lemenkova, P. 2020a. Visualization of the geophysical settings in the Philippine Sea margins by means of GMT and ISC data. Central European Journal of Geography and Sustainable Development, 2(1): 5-15. https://doi.org/10.47246/CEJGSD.2020.2.1.1.

Lemenkova, P. 2020b. GEBCO and ETOPO1 gridded datasets for GMT based cartographic mapping of Hikurangi, Puysegur and Hjort Trenches, New Zealand. Acta Universitatis Lodziensis. Folia Geographica Physica 19, 7–18. https://doi.org/10.18778/1427-9711.19.01.

Lemenkova, P. 2020c. GEBCO Gridded Bathymetric Datasets for Mapping Japan Trench Geomorphology by Means of GMT Scripting Toolset. Geodesy and Cartography 46 (3), 98–112. https://doi.org/10.3846/gac.2020.11524.

Lemenkova, P. 2020d. Fractal surfaces of synthetical DEM generated by GRASS GIS module r.surf.fractal from ETOPO1 raster grid. Journal of Geodesy and Geoinformation, vol. 7(1): 86–102. https://doi.org/10.9733/JGG.2020R0006.E.

Lemenkova, P. 2020e. Applying Automatic Mapping Processing by GMT to Bathymetric and Geophysical Data: Cascadia Subduction Zone, Pacific Ocean. Journal of Environmental Geography, 13(3-4): 15-26. https://doi.org/10.2478/jengeo-2020-0008.

Lemenkova, P. 2020f. Scripting cartographic methods of GMT for mapping the New Britain and San Cristobal Trenches, Solomon Sea, Papua New Guinea. Revista da Casa da Geografia de Sobral, 22(3), 122–142. https://doi.org/10.35701/rcgs.v22n3.717.

Lemenkova, P. 2020g. GRASS GIS Modules for Topographic and Geophysical Analysis of the ETOPO1 DEM and Raster Data: North Fiji Basin, Pacific Ocean. Geographia Napocensis, 14(1), 27-38. https://doi.org/10.6084/m9.figshare.13337318.

Lemenkova, P. 2020h. GRASS GIS for classification of Landsat TM images by maximum likelihood discriminant analysis: Tokyo area, Japan. Geodetski glasnik 51, 5–25. https://doi.org/10.6084/m9.figshare.13507761.

Lemenkova, P. 2019a. Processing Oceanographic Data ay Python Libraries Numpy, Scipy and Pandas. Aquatic Research, 2(2), 73-91. https://doi.org/10.3153/AR19009.

Lemenkova, P. 2019b. Statistical Analysis of the Mariana Trench Geomorphology Using R Programming Language. Geodesy and Cartography, 45(2), 57–84. https://doi.org/10.3846/gac.2019.3785.

Lemenkova, P. 2019c. Calculating slope gradient variations in the submarine landforms by R and Python statistical libraries. MANAS Journal of Engineering 7 (2), 99–113. https://doi.org/10.6084/m9.figshare.11454768.

Lemenkova, P. 2019d. GMT Based Comparative Analysis and Geomorphological Mapping of the Kermadec and Tonga Trenches, Southwest Pacific Ocean. Geographia Technica, 14(2), 39–48. https://doi.org/10.21163/GT_2019.142.04.

Lemenkova, P. 2019e. Topographic surface modelling using raster grid datasets by GMT: example of the Kuril-Kamchatka Trench, Pacific Ocean. Reports on Geodesy and Geoinformatics, 108, 9–22. https://doi.org/10.2478/rgg-2019-0008.

Lemenkova, P. 2019f. Regression Models by Gretl and R Statistical Packages for Data Analysis in Marine Geology. International Journal of Environmental Trends, 3 (1), 39–59. https://doi.org/10.6084/m9.figshare.8313362.

Lemenkova, P. 2019g. AWK and GNU Octave Programming Languages Integrated with Generic Mapping Tools for Geomorphological Analysis. GeoScience Engineering, 65(4), 1–22. https://doi.org/10.35180/gse-2019-0020.

Lemenkova, P. 2018a. Factor Analysis by R Programming to Assess Variability Among Environmental Determinants of the Mariana Trench. Turkish Journal of Maritime and Marine Sciences, 4 (2), 146-155. https://doi.org/10.6084/m9.figshare.7358207.

Lemenkova, P. 2018b. R Scripting Libraries for Comparative Analysis of the Correlation Methods to Identify Factors Affecting Mariana Trench Formation. Journal of Marine Technology and Environment, 2. https://doi.org/10.6084/m9.figshare.7434167.

Lemenkova, P. 2015a. Google Earth web service as a support for GIS mapping in geospatial research at universities. In: Web-technologies in the educational space, Problems, approaches, perspectives, 2, 460–464. https://doi.org/10.6084/m9.figshare.7211798.

Lemenkova, P. 2015b. Data Capture for Seafloor Bathymetric Mapping Using Software Caris Hips, GMT and ArcGIS. Actual Problems of the Modern Machinery, 111–117. https://doi.org/10.6084/m9.figshare.7210307.

Lemenkova, P., Promper, C., Glade, T. 2012. Economic Assessment of Landslide Risk for the Waidhofen a.d. Ybbs Region, Alpine Foreland, Lower Austria. In: 11th International Symposium on Landslides & the 2nd North American Symposium on Landslides & Engineered Slopes. NASL, Protecting Society through Improved Understanding. June 2–8, 2012. Banff, AB, Canada, 279–285. https://doi.org/10.6084/m9.figshare.7434230.

Lemenkova, P. 2011. Seagrass Mapping and Monitoring Along the Coasts of Crete, Greece. M.Sc. Thesis. Netherlands: University of Twente. 158 https://doi.org/10.13140/RG.2.2.16945.22881.

Mann, P., Taira, A. 2004. Global tectonic significance of the Solomon Islands and Ontong Java Plateau collision zone. Tectonophysics, 389, 137-190, https://doi.org/10.1016/j.tecto.2003.10.024.

Marchese, E., Scorpio, V., Fuller, I., McColl, S., Comiti, F. 2017. Morphological changes in Alpine rivers following the end of the Little Ice Age. Geomorphology, 295, 811–826. https://doi.org/10.1016/j.geomorph.2017.07.018.

Sandwell, D.T., Smith, W,H.F. 1997. Marine gravity anomaly from Geosat and ERS 1 satellite altimetry. Journal of Geophysical Research, 102(B5), 10039–10054. https://doi.org/10.1029/96JB03223.

Schenke, H. W., Lemenkova, P. 2008. Zur Frage der Meeresboden-Kartographie: Die Nutzung von AutoTrace Digitizer für die Vektorisierung der Bathymetrischen Daten in der Petschora-See. Hydrographische Nachrichten, 81, 16–21. https://doi.org/10.6084/m9.figshare.7435538.

Shiobara, H., Sugioka, H., Mochizuki, K., Oki, S., Kanazawa, T., Fukao, Y., Suyehiro, K. 2010. Double seismic zone in the North Mariana region revealed by long-term ocean bottom array observation. Geophysical Journal International, 183(3), 1455–1469.

Suetova, I. A., Ushakova L. A., Lemenkova, P. 2005. Geoinformation mapping of the Barents and Pechora Seas. Geography and Natural Resources, 4, 138–142. https://doi.org/10.6084/m9.figshare.7435535.

Wessel, P., Smith, W.H.F. 1995. New version of the Generic Mapping Tools released, EOS Trans. AGU, 76, 329.

http://topex.ucsd.edu/cgi-bin/get_data.cgi.